Measurement of femtosecond Polarization Mode Dispersion (PMD) using biased π-shifted low-coherence interferometry

E. Simova, I. Powell and C. P. Grover

National Research Council, INMS, Montreal Rd., Build. M-36, Ottawa, Ont. K1A 0R6, Canada
e-mail: eli.simova@nrc.ca ; ian.powell@nrc.ca;

Abstract: Conventional low-coherence interferometry (LCI) can be employed in the measurement of polarization mode dispersion (PMD) of fiber-optic components and fibers. However, the smallest PMD, which can be measured using this technique, is limited by the coherence length of the source. We propose a biased π-shifted Michelson interferometer where a birefringent crystal is inserted in front of the interferometer to introduce a bias differential group delay (DGD) larger than the coherence time of the source. In this way, the limitation imposed by the source coherence time has been overcome and PMDs much smaller than the source coherence time, in the order of several femtoseconds, can be measured. Experimental results for the PMD have been shown and compared with Jones matrix eigen-analysis. The theoretical model confirms the experimental observations.

OCIS codes: (060.2340) Fiber Optics Measurements

References

1. TIA/EIA Standard, FOTP-124, "Polarization Mode Dispersion Measurement for Single-Mode Optical Fibres by Interferometric Method," Aug., 1996.
2. P. Hernday, "Fibre Optic Test and Measurement," Ed. D. Derickson, (Prentice Hall, N. J. 1998), Ch. 10 and 12.
3. Y. Namihira, K. Nakajima and T. Kawazawa,, "Fully Automated Interferometric PMD Measurements for Active EDFA, Fibre-optic Components and Optical fibres," Electron. Letters, **29**, 18, 1649-1650 (993).
4. P. Oberson, K. Juilliard, N. Gisin, R. Passy and J. P. von der Weid, "Interferometric Polarization Mode Dispersion Measurements with Femtosecond Sensitivity", J. Lightwave Tech., **15**, 10, 1852 (1997).
5. P. Martin, G. LeBoudec, E. Tauflieb, and H. Lefevre, "Optimized Polarization Mode Dispersion Measurement with "π-shifted" White Light Interferometry," Opt. Fiber Technology, **2**, 207-212 (1996).
6. C. D. Poole and R. E. Wagner, "Phenomenological Approach to Polarization Mode Dispersion in Long Single-mode Fibers," Elect. Lett., **22**, 19, 1029 (1986).
7. D. S. Kliger, J. W. Lewis, C. E. Randall, "Polarized Light in Optics and Spectroscopy," (Academic Press Inc., 1990), Ch. 4 and 5.
8. B. L. Heffner, "Automatic measurement of polarization mode dispersion using Jones Matrix Eigenanalysis," IEEE Ph. Tech. Let., **4**, 1066-1069 (1992).

1. Introduction

Polarization mode dispersion (PMD) is known to be a limiting factor for long-distance wide-bandwidth transmission fiber links, since birefringence in fiber-optic components and fibers causes pulse broadening.

The interferometric method based on low-coherence interferometry (LCI) is a powerful tool to measure the PMD of fiber-optic components and fibers [1, 2]. The method usually uses a Michelson or Mach-Zehnder interferometer and provides a time-domain PMD measurement that is well suited for field measurements and production control. It has good dynamic range which is dependent on the travel range and step resolution of the scanning arm. The smallest PMD that can be measured is limited by the coherence length of the source because it imposes the minimum width on the interference pattern. The measurement

#23168 - $15.00 US Received July 26, 2000; Revised September 07, 2000

sensitivity is usually in the order of 100 fs, although smaller values have been reported [3]. For improved sensitivity, a broadband source is required to shorten the coherence length and sharpen the autocorrelation peak, but such sources usually have limited power output. This LCI method does not provide information about the Principal States of Polarization (PSPs) of device under test (DUT). An improvement of the interferometric technique towards measuring with a femtosecond sensitivity has been proposed in [4] by using a piece of highly birefringent (Hi-Bi) fiber. Difficulties with this arrangement arise from the fact that the central autocorrelation peak is always present and very strong, while the interference of the polarization modes results in much smaller side peaks. Another improvement to the Michelson interferometer has been suggested in [5] where a quarter waveplate (QWP) is inserted in one arm of the interferometer to suppress the central autocorrelation peak of the source. One common difficulty with the interferometric method is its sensitivity to the launched polarization. It may happen that only one polarization gets excited in the DUT or the Hi-Bi fiber and the two side peaks cannot be observed.

We propose a biased π-shifted Michelson interferometer where a birefringent crystal (biasing crystal) has been inserted in front of the interferometer to introduce a bias differential group delay (DGD) due to polarization larger than the coherence time of the source and thus overcome the limitation it imposes on the measurement sensitivity. Using this technique, PMD of devices smaller than the source coherence time, in the order of several fs, can be measured. The interferometer has a QWP inserted in the fixed arm, which introduces a π-shift in the passing polarizations. Thus in the interference pattern, the unwanted central autocorrelation peak is eliminated and the performance of the interferometer is improved. The biasing crystal and π-shift combination increases the resolution of the interferometer and lowers the minimum PMD that one can measure. Experimental results have been presented and compared with Jones matrix eigenanalysis. It is clearly seen that the experimental observations agree well with the theoretical model.

2. Representation of the biased π-shifted Michelson interferometer

The biased π-shifted Michelson interferometer is shown in Fig. 1. The polarization controller polarizes the light coming from the source, which is normally non-polarized. It also serves to set the input polarization to circular, in order to ensure that both polarization modes of the fiber-optic DUT are equally excited. When a DUT in weak mode-coupling regime is measured, the input polarized light is split into two polarization modes propagating along the axes of the PSPs with different velocities. At the output of the DUT these polarization states recombine with a DGD between them caused by the PMD of the DUT. When one mirror is scanned, the output response of the interferometer consists of three peaks, a central peak corresponding to the autocorrelation peak and two side peaks with the distance between them proportional to the DGD due to polarization in the DUT. The QWP is inserted in the fixed arm to eliminate the autocorrelation peak, thereby improving the system's signal sensitivity.

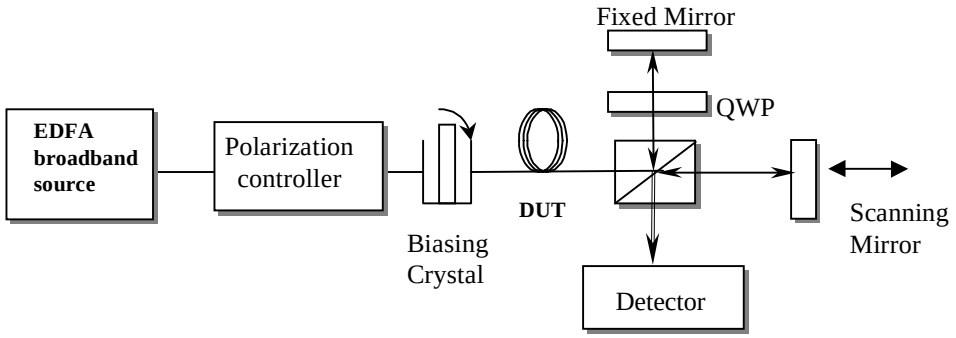

Fig. 1. Schematics of the biased π-shifted Michelson interferometer.

#23168 - $15.00 US Received July 26, 2000; Revised September 07, 2000

When circular polarization enters the set-up, and the PSPs and the axes of the QWP are aligned at 45 deg, the central peak is extinguished. The biasing crystal is inserted in front of the interferometer to introduce a DGD much larger than the coherence time of the source. When a broadband source, such as Light-Emitting Diode (LED) or EDFA-based white light source, is used, the first-order PMD of the DUT, $\Delta\tau$, is simply determined by the scanned distance, *2L*, between the two side peaks divided by the speed of light.

We assume that the DGD introduced by the DUT is smaller or equal to the coherence time of the source, $\Delta\tau_{DUT} \le \tau_{coh}$, and that it cannot be resolved by the interferometer. We consider a linearly birefringent fiber-optic DUT without polarization dependent loss (PDL). For a given input polarization state, the output polarization from the DUT depends generally on the optical angular frequency ω. Nevertheless, there are always two input polarization states such that the output polarization is, to a first order, independent of the wavelength [7]. These two principal states of polarization are orthogonal and correspond to the maximum and minimum propagation time through the medium. For the sake of simplicity, we also consider circular polarization entering the biasing crystal or the DUT. An angular parameter ρ is introduced to represent the misalignment of one component's PSPs or polarization axes relative to those of the other components in the interferometer. The results presented here can readily be generalized for a DUT with PDL and for an elliptical input polarization. Throughout the work, we use DGD due to polarization interchangeably with first-order PMD.

First, we consider the case when there is only a biasing crystal and a QWP in one arm of the interferometer (this configuration has been proposed in [5] with a DUT in place of the crystal). The crystal used to bias the interferometer is a uni-axial crystal with an *x*- or *y*-cut, so that the light travels perpendicular to the optic axis and a specific DGD for the o- and e-rays is introduced. According to the Jones matrix formalism [6], the transfer matrix of the crystal J_{crys}. in its coordinate system is given by

$$J_{crys.} = \begin{vmatrix} e^{i\frac{\delta}{2}} & 0 \\ 0 & e^{-i\frac{\delta}{2}} \end{vmatrix} \tag{1}$$

where δ is the optical phase difference (OPD) between the o- and e-rays propagating in the crystal.

We assume that the QWP in the fixed arm of the interferometer can have any alignment with respect to the crystal axes, i.e., at an arbitrary angle ρ. The Jones matrix of the QWP is given by:

$$J_{QWP} = \begin{vmatrix} e^{i\frac{\pi}{4}}\cos^2\rho + e^{-i\frac{\pi}{4}}\sin^2\rho & \sqrt{2}\sin\rho\cos\rho \\ \sqrt{2}\sin\rho\cos\rho & e^{-i\frac{\pi}{4}}\cos^2\rho + e^{i\frac{\pi}{4}}\sin^2\rho \end{vmatrix}. \tag{2}$$

The input field $\vec{E}(t)$ is split by the beamsplitter into two fields that pass through the scanning $\vec{E}_1(t)$ and the fixed $\vec{E}_2(t)$ arms of the interferometer. When the scanning arm is moved away from the beamsplitter by a distance $L/2$, the field in that arm $\vec{E}_1(t-\tau)$ is delayed by $\tau = L/c$ with respect to the field in the fixed arm $\vec{E}_2(t)$. When the mirror in the scanning arm is continuously translated, the optical detector detects the interference pattern resulting from the interference of the two fields in the following form:

$$I(\tau) \propto \left\langle \vec{E}_1(t-\tau) \right\rangle^2 + \left\langle \vec{E}_2(t) \right\rangle^2 + \left\langle \vec{E}_1(t-\tau)^* \vec{E}_2(t) \right\rangle e^{-i\varpi\tau} + \left\langle \vec{E}_1(t-\tau)\vec{E}_2(t)^* \right\rangle e^{i\varpi\tau} \tag{3}$$

#23168 - $15.00 US Received July 26, 2000; Revised September 07, 2000

where the indices 1 and 2 denote the field passing through the scanning and fixed arms, respectively, the brackets denote time averaging carried out by the detector, ϖ is the average optical frequency of the radiation, and the asterix (*) denotes the complex conjugate of the amplitudes associated with the electric field vector. The last two terms in Eq. (3) contain the information about the interference pattern and have the form of first-order correlation. Using the fact that the Fourier transformation of the correlation of two signals is equal to the product of their Fourier transforms, the interference terms in Eq. (3) can also be written as

$$I \propto \int_{-\infty}^{\infty} d\omega \int_{-\infty}^{\infty} d\omega' \left\langle \tilde{\tilde{E}}_1(\omega, L)\tilde{\tilde{E}}_2^{*}(\omega', L) \right\rangle . \tag{4}$$

The tilde-symbol ($\tilde{}$) denotes the Fourier transform with

$$\tilde{\tilde{E}}_1(\omega) = \tilde{\tilde{E}}_{in}(\omega) T_1(\omega)\vec{e}_1 \text{ and } \tilde{\tilde{E}}_2(\omega) = \tilde{\tilde{E}}_{in}(\omega) T_2(\omega)\vec{e}_2 \tag{5}$$

where $\tilde{\tilde{E}}_{in}(\omega)$ is the Fourier transform of the source signal, $T_1(\omega)$ and $T_2(\omega)$ are the transfer functions for the scanning and fixed arms respectively, $\vec{e}_1$ and $\vec{e}_2$ account for the polarization states of the two fields. The quantity $\left\langle \tilde{\tilde{E}}_{in}(\omega)\tilde{\tilde{E}}_{in}^{*}(\omega') \right\rangle = 2\pi\delta(\omega - \omega')\tilde{\Gamma}(\omega)$ where $\tilde{\Gamma}(\omega)$ is the autocorrelation function of the source. For the case of LCI, the light source is emitting in a wavelength bandwidth of $\Delta\omega = -(2\pi c/\lambda^2)\Delta\lambda$ and the source autocorrelation function has a Gaussian shape determined by the spontaneous emission. Therefore, the final form of the interference term is multiplied by an envelope function in the form of $\exp\left[-(2\Delta L/L_{coh})^2\right] = \exp\left[-(2\Delta\tau/\tau_{coh})^2\right]$, where ΔL refers to the OPD and $\Delta\tau$ to the DGD accumulated by the light radiation passing through the interferometer arms, while L_{coh} and τ_{coh} refer to the source coherence length and time respectively.

Having introduced the source coherence time, we now return to the Jones calculus. For convenience, we allow the directions of the "fast" and "slow" polarization modes to be aligned with the x- and y-axes respectively. When the biasing crystal introduces DGD, $\Delta\tau_{crys.}$, between its "fast" and "slow" component along its polarization axes much larger than the source coherence time, i.e., $\Delta\tau_{crys.} \succ \tau_{coh}$, the two waves exiting the crystal recombine incoherently. There is no coupling between them and they propagate through the arms of the interferometer independently as: $E_{1x}(t-\tau)$ and $E_{1y}(t-\tau)$ in the scanning arm and as $E_{2x}(t)$ and $E_{2y}(t)$ in the fixed arm respectively. Therefore, the Jones vector $(E_x(t),\ E_y(t))$ can now be treated as two separate vectors $(E_x(t),\ 0)$ and $(0,\ E_y(t))$ at the exit of the crystal. In both arms there is one reflection taking place, either from the moving or fixed mirror. Furthermore, in the stationary arm, the radiation passes through the QWP twice. At the exit of the interferometer in the vicinity of the detector surface, the propagating waves have the form:

$$\vec{E}_1(t-\tau) = \begin{pmatrix} E_{1x}(t-\tau) \\ 0 \end{pmatrix} + \begin{pmatrix} 0 \\ E_{1y}(t-\tau) \end{pmatrix} = J_{crys.} \begin{pmatrix} Ae^{i\phi} \\ Ae^{i\phi+\pi/2} \end{pmatrix} e^{i\pi + \frac{2\pi i}{\lambda} L}$$

$$\vec{E}_2(t) = \begin{pmatrix} E_{2x}(t) \\ 0 \end{pmatrix} + \begin{pmatrix} 0 \\ E_{2y}(t) \end{pmatrix} = J_{QWP}^2 J_{crys.} \begin{pmatrix} Ae^{i\phi} \\ Ae^{i\phi+\pi/2} \end{pmatrix} e^{i\pi} . \tag{6}$$

After substituting Eqs. (6) into Eq. (3), the interference term can be obtained:

#23168 - $15.00 US Received July 26, 2000; Revised September 07, 2000

$$I \propto 2|A|^2 \exp\left[-\left(\frac{2\Delta\tau}{\tau_{coh}}\right)^2\right]\left\{\sin(2\rho)\left[\cos\left(\frac{2\pi}{\bar{\lambda}}L-\delta\right)+\cos\left(\frac{2\pi}{\bar{\lambda}}L+\delta\right)\right]+ 2\cos(2\rho)\sin\left(\frac{2\pi}{\bar{\lambda}}L\right)\right\} \quad (7)$$

As can be seen from Eq. (7), when the angle ρ between the crystal axes and the QWP is zero, $\cos(2\rho)=1;\sin(2\rho)=0$, only the source autocorrelation peak is present in the interference pattern and the information about DGD of the biasing crystal is lost. When the QWP is aligned at ρ = *45* deg, $\cos(2\rho)=0;\sin(2\rho)=1$, there are two peaks corresponding to the interference from the "slow" and "fast" polarization modes and the central autocorrelation peak is extinguished. From Eq. (7), the DGD due to polarization (or PMD) introduced by the crystal (or any DUT in the weak-mode coupling regime) can be calculated as:

$$\Delta\tau = \frac{2L}{c} \quad (8)$$

where *2L* is the scanned distance between the maxima of the two peaks, and *c* is the speed of the light. In the LCI, Eq. (8) is used to calculate the PMD in fiber-optic devices according to [3, 5]. It is easily appreciated that a limitation exists with this configuration when $\Delta\tau_{DUT} \le \tau_{coh}$. Under this condition the two peaks in Eq. (7) produce only one broadened peak in the fringe pattern and therefore cannot be resolved. With our proposed biased π-shifted configuration, having aligned the crystal and the QWP at 45 deg relative to each other, a reference scan is performed to determine precisely the biasing DGD, $\Delta\tau_{crys}$. The precise alignment is assured by the full elimination of the central autocorrelation peak. Equation (8) is also used to calculate the DGD of the biasing crystal.

Next, we consider the case, when a DUT is connected to the biased π-shifted interferometer in front of the crystal. A pictorial representation of the polarized light waves passing through the DUT and the crystal, as well as the accumulated DGDs, is illustrated in Fig. 2. For the sake of clarity, circular polarization is assumed to enter the crystal and the QWP is not shown. The angular misalignment ρ is shown for the crystal rather than the DUT. Since $\Delta\tau_{DUT} \le \tau_{coh}$ has been assumed, the radiation exiting the DUT with mutually perpendicular PSPs recombines coherently. This changes the resultant output polarization to elliptical and broadens the resulting wave train. Upon entering the biasing crystal, the wave

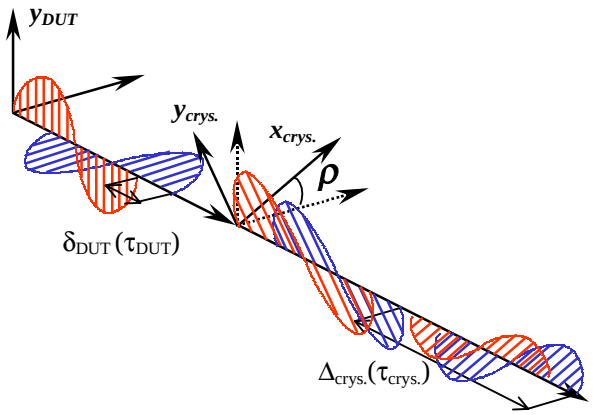

Fig. 2. Pictorial representation of the polarized light waves passing through the DUT and the biasing crystal where the DUT's and the crystal's axes are misaligned by an angle ρ.

#23168 - $15.00 US Received July 26, 2000; Revised September 07, 2000

train splits along the crystal polarization axes. At the crystal exit, since $\Delta\tau_{crys.} \succ \tau_{coh}$, the waves with perpendicular polarizations accumulate OPD much larger than the source coherence length. The two waves recombine incoherently and propagate through the interferometer without any phase relationship between them. The biasing crystal and QWP are assumed aligned at 45 deg and hence the central autocorrelation peak is suppressed. The DUT is considered as a linear retarder with an OPD, Δ, introduced between the two polarization modes with axes at an arbitrary angle, ρ, relative to the crystal axes. It can be represented by its Jones matrix as:

$$J_{DUT} = \begin{vmatrix} e^{i\frac{\Delta}{2}}\cos^2\rho + e^{-i\frac{\Delta}{2}}\sin^2\rho & 2\sin\rho\cos\rho\sin\frac{\Delta}{2} \\ 2\sin\rho\cos\rho\sin\frac{\Delta}{2} & e^{-i\frac{\Delta}{2}}\cos^2\rho + e^{i\frac{\Delta}{2}}\sin^2\rho \end{vmatrix}. \tag{9}$$

The waves propagating through the two arms of the interferometer and reaching the detector surface, which have been represented by Eqs. (6), now take the form:

$$\begin{aligned} \vec{E}_1(t-\tau) &= \begin{pmatrix} E_{1x}(t-\tau) \\ 0 \end{pmatrix} + \begin{pmatrix} 0 \\ E_{1y}(t-\tau) \end{pmatrix} = J_{crys.}J_{DUT}\begin{pmatrix} Ae^{i\phi} \\ Ae^{i\phi+\pi/2} \end{pmatrix} e^{i\pi+\frac{2\pi i}{\bar{\lambda}}L} \\ \vec{E}_2(t) &= \begin{pmatrix} E_{2x}(t) \\ 0 \end{pmatrix} + \begin{pmatrix} 0 \\ E_{2y}(t) \end{pmatrix} = J_{QWP}^2 J_{crys.}J_{DUT}\begin{pmatrix} Ae^{i\phi} \\ Ae^{i\phi+\pi/2} \end{pmatrix} e^{i\pi}. \end{aligned} \tag{10}$$

Substituting Eqs. (10) into Eq. (3), the final form of the interference term can be obtained as:

$$\begin{aligned} I \propto 2|A|^2 \exp\left[-\left(\frac{2\Delta\tau}{\tau_{coh}}\right)^2\right]\Bigg\{ & \sin^2\rho\left[\cos\left(\frac{2\pi}{\bar{\lambda}}L-(\delta-\Delta)\right)+\cos\left(\frac{2\pi}{\bar{\lambda}}L+(\delta-\Delta)\right)\right]+ \\ & \cos^2\rho\left[\cos\left(\frac{2\pi}{\bar{\lambda}}L-(\delta+\Delta)\right)+\cos\left(\frac{2\pi}{\bar{\lambda}}L+(\delta+\Delta)\right)\right] \end{aligned}. \tag{11}$$

It should be noted that in this case, there is no central autocorrelation peak. As can be seen from Eq. (11), when $\rho = 0$ deg, i.e., $\cos^2\rho = 1$, the DUT's polarization (PSPs) are aligned with those of the crystal and the DGDs introduced by the DUT and the crystal are summed up. When $\rho = 90$, i.e., $\sin^2\rho = 1$, the "fast" axis of the DUT is aligned with the "slow" axis of the biasing crystal and vice versa and the two delays get subtracted. In both cases, there are two distinct well-separated peaks in the interference pattern resulting from the large DGD of the crystal. Hence, the PMD of the DUT can be obtained by the relative shift in the peaks' positions from their nominal positions in the reference scan rather than by the separation of peaks it introduces. In the case of $\rho = 45$ deg, the sum and the difference of the DGDs are both present resulting in broadening of the peaks, if they cannot be resolved.

Several scans need to be carried out with the DUT in front of the biasing crystal to determine the alignment positions where the DGDs of the biasing crystal and the DUT sum up and subtract. Normally, the DUT has fixed PSPs, and therefore, the crystal and QWP combination should be re-adjusted to achieve either $\rho = 0$ or 90 deg. Having determined either of said orientations, results from the scans would yield the combined DGD from Eq. (8), $\Delta\tau_{crys\pm DUT}$, while together with the scan carried out previously for just the crystal would allow the DGD associated with the DUT to be calculated as

#23168 - $15.00 US Received July 26, 2000; Revised September 07, 2000

$$\Delta\tau_{DUT} = \Delta\tau_{crys.\pm DUT} - \Delta\tau_{crys.}\,. \tag{12}$$

Somewhat more precisely, the $\Delta\tau_{DUT}$ can be determined from two consecutive scans where $\rho = 0$ or $\rho = 90$ deg, and the DGDs of the DUT and the crystal add up and subtract. Then the DUT's DGD can be calculated from Eqs. (8) and (11) as

$$\Delta\bar{\tau}_{DUT} = \left(\Delta\tau^{+}_{DUT} + \Delta\tau^{-}_{DUT}\right)\!/2\,. \tag{13}$$

3. Measurements

The measurements of DGDs due to polarization were carried out in the interferometric set-up shown in Fig. 1. The optical source used in the experiments was an EDFA-based broadband source with a central wavelength of $\bar{\lambda} = 1530$ nm and a bandwidth (FWHM) of $\Delta\lambda = 42$ nm at –10 dB. The source coherence length was $L_{coh} = \bar{\lambda}^2/\Delta\lambda \approx 56\ \mu$m Therefore, without the bias, the interferometer was limited to measuring $\Delta\tau_{DUT} \approx \tau_{coh} \approx 0.18$ ps. With the biasing crystal, this limitation was overcome and smaller DGDs were measured by the relative shifts of the two peaks from their nominal positions when only the crystal was present (according to Eqs. (8), (12) and (13)). The biasing crystal was an y-cut $LiNiO_3$. When circular polarization entered the crystal, the accurate alignment between the crystal and the QWP was achieved when the central peak was extinguished (according Eq. (7)). The QWP was then kept aligned at 45 deg to the crystal axes all throughout the experiments. First, a reference scan was carried out with the biasing crystal aligned at 45 deg to the QWP. The crystal DGD was evaluated from the recorded interference pattern according to Eq. (8) to yield $\Delta\tau_{crys.} = 2.706\ ps$. The measured DGD was verified with the Jones Matrix Eigenanalysis (JME) method where the averaged DGD was obtained over the wavelength range of the broadband source. The JME method gave a value of $\Delta\tau_{crys.} = 2.688$ ps. The agreement between the results measured by the two methods is 0.018 ps, i.e., within 1%. The wavelength scan of the DGD due to polarization for the bias crystal from the JME method is depicted in Fig. 3.

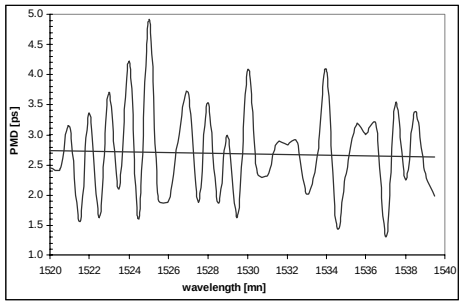

Fig. 3. Measured DGD due to polarization for the bias crystal using the Jones Matrix Eigenanalysis method.

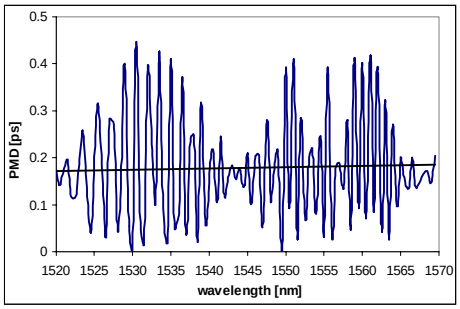

Fig. 5. Measured DGD for the second crystal (DUT) using the Jones Matrix Eigenanalysis method.

To validate the proposed measurement method and theoretical model, a second crystal with a small delay, $\Delta\tau_{DUT} \approx \tau_{coh}$, was introduced as the DUT with rotateable polarization axes, i.e., the angular misalignment ρ could be varied without varying the introduced DGD. The interference patterns resulting from when the DUT was introduced upstream from the biasing crystal are presented in Fig. 4. To facilitate the comparison between the between the different interference patterns, all scans have been shown in the same figure. The navy blue line presents the reference scan with the bias crystal only (to be compared with Fig. 3); the pink plot represents the case when the DUT polarization axes are aligned with those of the bias crystal *(ρ = 0* deg) and the DGDs of the DUT and crystal are summed up; the light blue plot

#23168 - $15.00 US Received July 26, 2000; Revised September 07, 2000

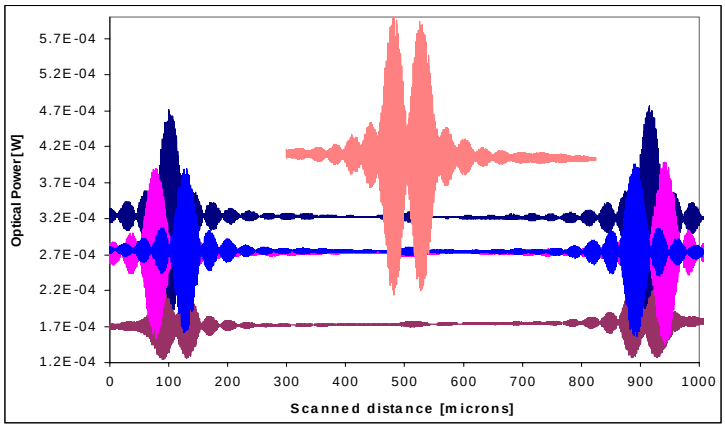

Fig. 4. Interference patterns obtained from the biased π-shifted Michelson interferometer in the case of a second crystal with rotateable axes used as DUT: navy blue line – reference scan with the bias crystal only; pink line – DUT, polarization axes aligned with those of the bias crystal ($\rho=0$ deg); light blue line - DUT polarization axes crossed with those of the bias crystal ($\rho = 90$ deg); reddish-brown line – DUT polarization axes at an arbitrary angle ($\rho = 45$ deg). For comparison, the orange line in the center represents fringe pattern resulting from the DUT only without the bias.

shows the case when the DUT polarization axes are crossed with those of the bias crystal ($\rho = 90$ deg), that is the "fast" and "slow" PSPs of the DUT are aligned with the "slow" and "fast" axes of the crystal, respectively, and the DGDs of the DUT and the crystal subtract; the brown plot shows the scan for the DUT polarization axes at an arbitrary angle ($\rho \sim 45$ deg). For comparison, the red plot in the centre depicts the interference pattern resulting from the DUT only without the bias crystal. The DGD of the second crystal used as DUT was calculated from Fig. 4 with Eqs. (8), (12) and (13) as $\Delta\tau_{DUT} = 0.179$ ps. For comparison, Fig. 5 illustrates the wavelength scan for the DGD from the JME method, which gives an average DGD for the DUT of $\Delta\tau_{DUT} = 0.177$ ps, an excellent agreement with the interferometric method within 2 fs or approximately 1%.

As a second example, the DGD due to polarization (PMD) of a fibre-optic circulator was also measured. With the interferometer being properly aligned to minimize the central peak, again a reference scan with the bias crystal was carried out first, then, with the DUT connected, a second scan was undertaken. The measurement results from both scans are presented in Fig. 6, where the reference scan is shown by the navy blue plot, and the scan with the DUT - with the pink plot. Generally, the DUT's PSPs are not aligned with the polarization

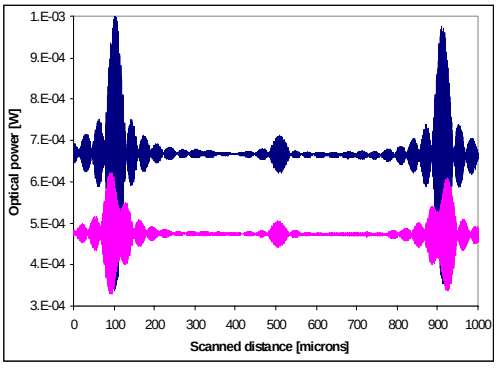

Fig. 6. Interference patterns for a fiber-optic circulator: navy blue line – reference scan with the bias crystal only; pink line – DUT, polarization axes misaligned with those of the bias crystal ($\rho \neq 0$ deg).

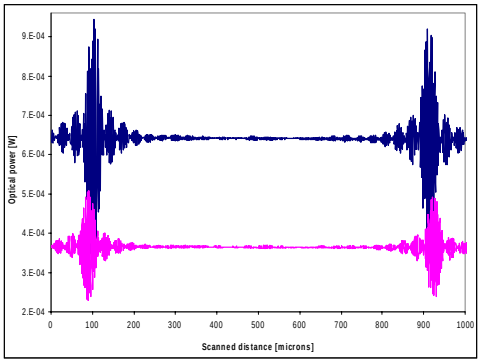

Fig. 7. Interference pattern for the fiber-optic circulator with its polarization axes aligned with those of the bias crystal ($\rho = 0$ deg): navy blue line – reference scan with the bias crystal; pink line – DUT.

#23168 - $15.00 US
Received July 26, 2000; Revised September 07, 2000

axes of the bias crystal and the QWP. This can be seen from the asymmetry in the side peaks associated with the DUT plot. It is apparent from the scanned fringe pattern that the DGDs of the DUT and the bias crystal are added up as phasors (or vectors). As a result, the value for the DGD, calculated as $\Delta\tau_{DUT} = 0.07\,\text{ps}$ from Eqs. (8) and (12), may be somewhat underestimated. This is the case, indeed, as it can be seen in Fig. 7, which shows the resulting fringe patterns for the bias crystal and the fiber-optic circulator after the crystal -QWP combination had been rotated as a unit to align the axes with those of the DUT. In the latter case, the value for the DUT's DGD from Eq. (8) and (12) gives $\Delta\tau_{DUT} = 0.077\,\text{ps}$. For comparison, the DGD of the fiber-optic circulator was obtained using the JME method and is shown in Fig. 8. The mean value for $\Delta\tau_{DUT} = 0.075\,\text{ps}$ indicates an agreement between the two methods of 2 fs, or to better than 3% difference.

The major sources of errors using the interferometric method arise from the coherence time of the light source, the launched state of polarization and the step resolution of the moving arm. The coherence time determines the width of the intensity peaks. Combined with the minimum step resolution of the moving arm, it determines the minimum measurable shift of the peaks from their nominal positions and therefore the smallest measurable value of PMD. In this configuration, we could determine the peaks position with an accuracy of ± 0.5 μm. For example, a 1 μm error in determining the peak position results in 3 fs error in determining the PMD, which would represent the minimum measurable PMD in the current configuration.

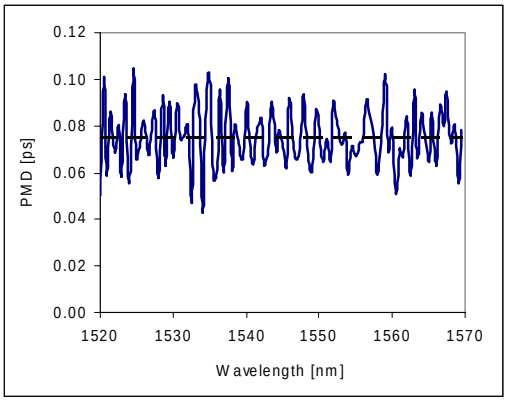

Fig. 8. Measured DGD for the fiber-optic circulator using the Jones Matrix Eigenanalysis method.

4. Conclusions

We have proposed and demonstrated a biased π-shifted Michelson interferometer for measuring PMD in the order of several femtoseconds. The interferometer has a quarter waveplate inserted in the fixed arm which eliminates the central autocorrelation peak of the source and thus increases the resolution of the interferometer and lowers the minimum PMD one can measure. The improvement over the existing instruments resulting from a birefringent crystal being inserted in front of the interferometer to introduce a bias DGD much larger than the coherence time of the source, thus overcoming the limitation imposed by it. With such bias, PMD of devices much smaller than the source coherence time can be measured. Experimental observations have been confirmed by the developed theoretical model. Experimental results have been presented and compared with Jones matrix eigenanalysis.

Acknowledgements

E. S. would like to thank Dr. K. Stoev for the many useful discussions and suggestions and for his interest in this work.

#23168 - $15.00 US Received July 26, 2000; Revised September 07, 2000